THE ASTROPHYSICAL JOURNAL, 401:353–360, 1992 December 10

FAR-INFRARED SPECTRAL STUDIES OF PHASE CHANGES IN WATER ICE INDUCED BY PROTON IRRADIATION

MARLA H. MOORE
Astrochemistry Branch, Laboratory for Extraterrestrial Physics, NASA/Goddard Space Flight Center, Greenbelt, MD 20771
AND
REGGIE L. HUDSON
Department of Chemistry, Eckerd College, St. Petersburg, FL 33733
Received 1992 February 28; accepted 1992 June 16

ABSTRACT

Far-infrared spectra from 20 μm (500 cm^{-1}) to 100 μm (100 cm^{-1}) of water ice have been measured over the temperature range of 13–155 K. Amorphous and crystalline water ice are easily identified in far-infrared spectra since amorphous ice has one broad absorption peak near 45 μm (220 cm^{-1}) and crystalline has absorptions near 44 μm (229 cm^{-1}) and 62 μm (162 cm^{-1}).

We have observed radiation-induced phase changes in both amorphous and crystalline ice. Crystalline ice converts to an amorphous phase when irradiated at temperatures between 77 and 13 K. The conversion rate increases as the temperature is decreased and the converted fraction is dose dependent. No radiation-induced changes are detected in amorphous ice between 125 and 36 K. However, far-infrared spectra of proton-irradiated ices near 13 K show interconversion between the amorphous and crystalline ice phases beginning at doses near 2 eV molecule^{-1} and continuing cyclically with increased dose. A quadrupole mass spectrometer was used to detect H_2, H_2O, and O_2 releases associated with the cyclic phase conversions.

Radiation-induced phase changes in these two forms will be discussed in relation to interstellar ices, and ices in comets.

Subject headings: dust, extinction — molecular data

1. INTRODUCTION

Recent far-infrared observations by Omont et al. (1990) of a circumstellar envelope of an evolved bipolar nebula (IRAS 09371+1212) show a 40–70 μm emission band which can be fitted with the spectra of crystalline water ice on crystalline silicate grains at 46 K; the ice spectrum has a sharp maximum near 45 μm and a weaker secondary maximum near 62 μm. The original identification of water ice in IRAS 09371+1212 was based on the large 3.1 μm absorption feature (Geballe et al. 1988; Hodapp, Sellgren, & Nagata 1988; Rouan et al. 1988). All interpretations support the presence of some crystalline ice. Similarly, a 3.1 μm feature has also been observed in two other bipolar nebulae, OH 231.8+4.2 (Smith, Sellgren, & Tokunaga 1988) and M1-92 (Eiroa & Hodapp 1988), and most interpretations of the spectra include crystalline ice. Condensation of some crystalline ice in an expanding circumstellar envelope (see, e.g., Jura & Morris 1985) is a different formation mechanism than the accretion of gas-phase atoms and molecules on low-temperature grains. The latter favors the formation of amorphous ice. Léger et al. (1983) pointed out that the spectrum of laboratory amorphous water ice fit the shape of the interstellar 3.1 μm absorption feature observed in the spectra of several dense molecular clouds. It is thought that interstellar ices existed in the interstellar cloud which collapsed to form our solar nebula.

Comets are thought to be formed of amorphous ice accreted from materials located in the outer part of the primordial solar nebula 4.6×10^9 yr ago. Since then they probably have remained at temperatures below 50 K while being stored in the Oort cloud region. But, during perihelion passage, crystallization of some of the compositionally complex "surface" amorphous ice probably occurs since the outer cometary layers are exposed to intense warming.

It has been suggested (Klinger 1983) that the determination of the physical state of ice in space may give information on the thermal history of extraterrestrial matter. Amorphous ice, once formed, is not stable against temperature cycling. It converts to the cubic crystalline phase, I_c, on a time scale which decreases with increasing temperature. Continued warming of I_c to $T > 170$ K (Hobbs 1974) results in its conversion to the crystalline hexagonal, I_h, phase.

The structure of crystalline ice, however, can be modified by both ultraviolet and particle irradiation. Kouchi & Kuroda (1990) studied the effect of ultraviolet radiation on I_c using electron diffraction to follow the structural changes. They found that below 70 K, ultraviolet irradiation transforms I_c into amorphous ice. Similar amorphization was detected by Lepault, Freeman, & Dubochet (1983) and Heide (1984) after electron exposure (100 keV) from a cryoelectron microscope. Strazzulla et al. (1991) and Strazzulla (1991) studied the amorphization of crystalline ice by monitoring spectral changes in the 3.1 μm water band as a function of 3 keV He^+ irradiation over the temperature range of 10–100 K. Baratta et al. (1991) applied the results to the 3.1 μm spectrum observed for the bipolar nebula OH 231.8+4.2.

We wanted to study the far-infrared 50–100 μm band of water ice as a function of irradiation since the difference between the amorphous and crystalline phase is well defined in this region, and because (unlike the 3.1 μm band) it is not coincident with absorptions due to molecules such as NH_3 and CH_4 which are often present in astronomically releavant icy mixtures. Spectral data of water ice in the far-infrared are more

limited than in the mid-infrared. Bertie & Whalley (1967) and Bertie, Labbé, & Whalley (1969) published far-infrared spectra to 200 μm (50 cm^{-1}) and absorption coefficients to 33 μm (30 cm^{-1}) respectively for 100 K crystalline H_2O ice. The far-infrared spectrum of I_h is indistinguishable from I_c at 90 K and shows only minor differences at 4.3 K (see Bertie & Jacobs 1977, and references therein). In general we refer to those forms as crystalline ice. Far-infrared spectra were observed at temperatures in the 90–250 K range during the phase transformation from amorphous to the crystalline phase (Hardin & Harvey 1973). There is, however, no published information on the thermal evolution of ice spectra in the far-infrared over the temperature range from 13 to 155 K. The optical constants of 77 K amorphous ice published by Léger et al. (1983) extended into the far-infrared to 77 μm (130 cm^{-1}). More recently, the n and k values to 200 μm (50 cm^{-1}) for amorphous ice deposited at 10 K along with the optical constants for amorphous ice at 100 and 140 K were determined (Hudgins et al. 1991).

In this paper we report on changes in the far-infrared spectrum of crystalline and amorphous H_2O ice as a function of temperature. We use the dramatic difference between the spectra of these ices in the far-infrared to examine the effect of proton irradiation on the stability of the crystalline and amorphous ice phase from 13 to 77 K. Results are used to estimate the stability of irradiated ices in astronomical environments.

2. EXPERIMENTAL PROCEDURE

Experiments were conducted on ices grown on an aluminum substrate (area ≈ 5 cm^2) cooled by a closed-cycle cryostat ($T_{min} \approx 13$ K). Surrounding the substrate was a six-sided chamber (see Fig. 1) designed to allow a variety of in situ measurements. Although Figure 1 shows the ice film facing the spectrometer, the ice could be rotated to face any direction. Infrared (IR) absorption spectra were recorded with a Mattson (Polaris) Fourier-transform infrared (FTIR) single-beam spectrometer equipped with a 6 μm Mylar beam splitter. Using a focus projection attachment, the IR beam was directed at a right angle to the spectrometer bench through a 16 mm thick high-density polyethylene window where it passed through the ice film, reflected at the ice-aluminum interface, and again passed through the ice film before traveling to the detector. This technique results in transmission-reflection-transmission spectra (TRT-spectra) which are recorded as 60 scan accumulations ($\sim$3 minute total accumulation time) from 20 μm to 100 μm (500–100 cm^{-1}) with a resolution of 4 cm^{-1}. Each single-beam spectrum was ratioed with a background spectrum. The optical path, except within the sample chamber, was purged with dry nitrogen gas during all experiments. Absorptions due to any residual water vapor within the optical path had minimal effect on the spectra if the background and single-beam spectra were recorded with the same purge conditions.

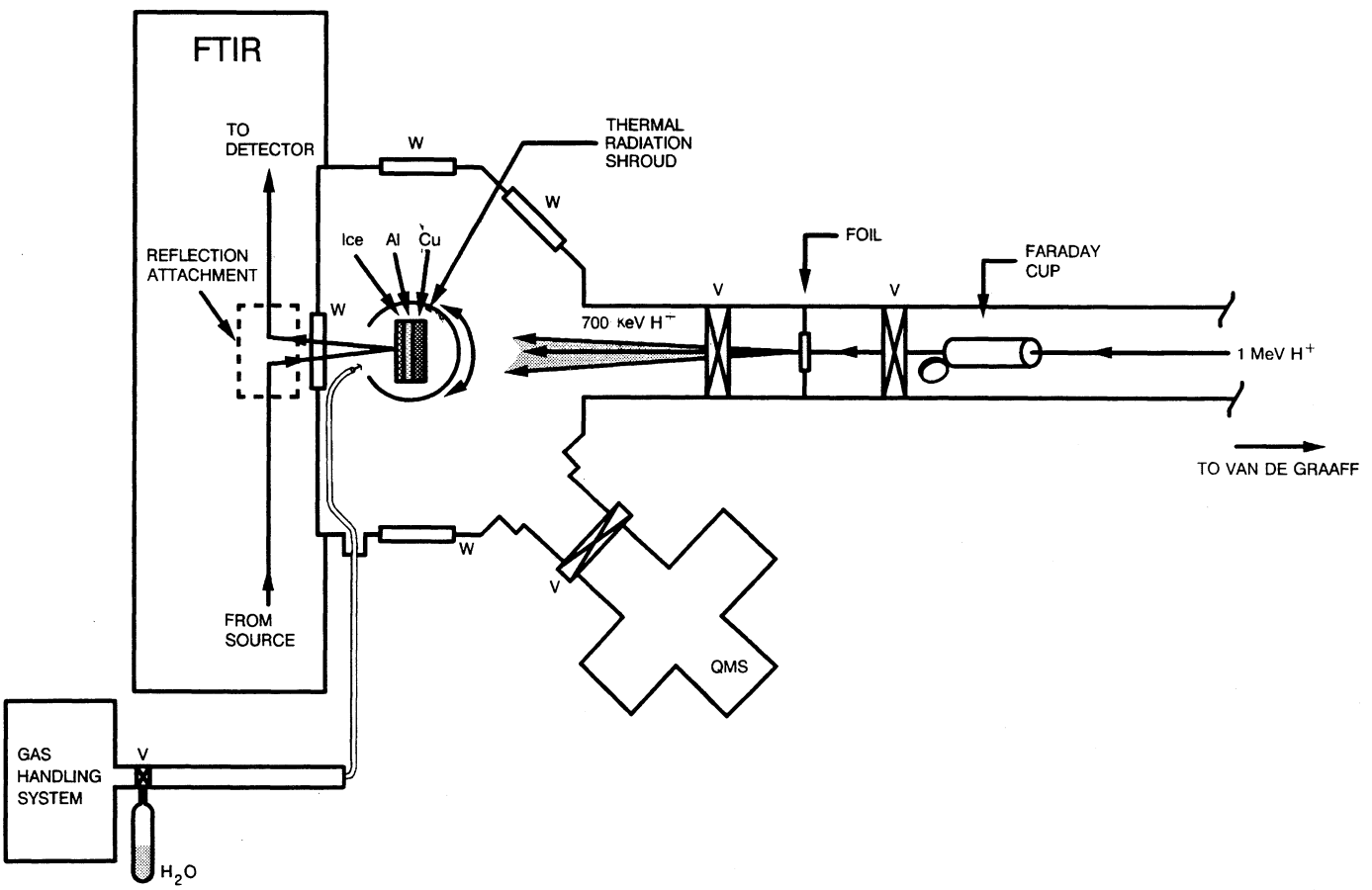

FIG. 1.—Schematic of experimental set up. The multiport chamber with several windows (W) is vacuum connected (V = vacuum valves) to the Van de Graaff accelerator. Infrared spectra of the ice are measured using the FTIR and species released from the ice during warming are detected using the quadrupole mass spectrometer (QMS).

The water used to make the ice samples was triply distilled with a resistance greater than 10^7 ohm-cm and with dissolved gases removed by freeze-pump-thaw cycles. Thin films of amorphous ice, about 4 μm in thickness, were grown at ~ 10 μm hr^{-1} by condensation of H_2O vapor onto the substrate precooled to 13 K. (Ices grown at rates down to 1 μm hr^{-1} gave the same spectra as those grown at 10 μm hr^{-1}.) To produce crystalline ice, amorphous ice was warmed from 13 to 155 K, held there about 5 minutes, and then cooled to the desired temperature.

The radiation source was a 1 MeV proton beam from a Van de Graaff accelerator. A Faraday cup, shown rotated out of the beam path in Figure 1, was used for beam alignment. The energy of the 1 MeV protons was degraded to 700 keV after passing through a nickel foil (Fig. 1), used to separate the accelerator and cryostat vacuum systems, preventing sample contamination. During irradiations the ice film was rotated 180° from the direction of the FTIR to face the radiation source. Since the range of 700 keV protons in water ice is about 13 μm, the beam passed completely through the ~ 4 μm thick ice before being stopped in the substrate. Although the aluminum substrate was thermally connected to the cryostat, it was electrically isolated. This allowed the substrate to be used as a second Faraday cup; the resulting integrated beam current was a direct measure of the incident fluence (p^+ cm^{-2}). The beam current at the substrate was typically 1×10^{-7} A.

Located at 45° to the proton beam line was a Dycor quadrupole mass spectrometer (QMS) (model M200M). It was used to detect volatile species released from the ice sample either during irradiation or during thermal cycling. The QMS range (m/z) (assuming $z = 1$) was 1 amu to 200 amu with a minimum detectable partial pressure less than 10^{-11} torr.

Irradiations of a blank substrate at 13 K gave neither detectable mass spectral nor temperature changes during the irradiation nor changes in the substrate's far-infrared reflectance.

3. RESULTS

In the far-infrared from 20 μm (400 cm^{-1}) to 100 μm (100 cm^{-1}) the difference between the spectra of amorphous and crystalline H_2O ice is more dramatic than at shorter wavelengths. Figure 2 compares the far-infrared spectrum of amorphous ice deposited at 13 K with the spectrum of that ice converted to the crystalline form by warming to 155 K and then recooling to 13 K. The absorptions at 44.8 μm (223 cm^{-1}) and at 63.3 μm (158 cm^{-1}) in the crystalline phase correspond to the transverse optical and longitudinal acoustic modes, respectively. Changes between the two ice phases are easy to detect and make it possible to examine the effects of temperature and radiation on the ice structure.

3.1. *Far-Infrared Spectra of Amorphous and Crystalline Ice as a Function of Temperature*

Amorphous ice has a single broad symmetrical band with a peak at 45.5 μm (220 cm^{-1}). X-ray data on low-temperature amorphous ice support the idea that it is a random network of hydrogen bonds which results in very short-range ordering. Two forms of amorphous ice have been reported (Narten, Venkatesh, & Rice 1976): a high-density (1.1 g cm^{-3}) form condensed at 10 K on a single crystal of Cu and a low-density (0.94 g cm^{-3}) form condensed at $T > 10$ K on a variety of substrates. We assume our ices are the low-density form.

We compared our 13 K amorphous spectrum with the only set of far-infrared optical constants available for amorphous ice near 13 K, determined by Hudgins et al. (1992) (referred to as HSAT). They formed amorphous ice on a polyethylene window and their transmission spectra were corrected for both reflection and interference effects. When our TRT spectra of amorphous ice are normalized to HSAT's absorption coefficients, the area of the two curves differ by $\sim 8\%$. Our data are reproducible from day-to-day within $\pm 2\%$. The reflectivity of amorphous ice calculated from HSAT's data is typically under 10% and the area of our normalized absorbance spectra is changed $\sim 6\%$ if corrections for reflection are made.

A sequence of far-infrared spectra in Figure 3 shows the thermal evolution of a 2.3 μm thick sample of amorphous H_2O deposited at 13 K. Each spectrum is recorded after warming the amorphous ice (rate ~ 5 K minute^{-1}) and holding the sample at that temperature for ~ 10 minutes. As the tem-

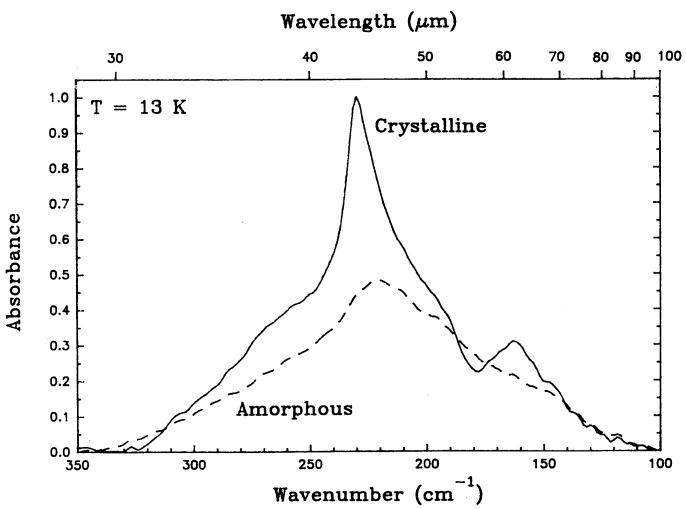

FIG. 2.—Comparison of the far-infrared spectrum of a 4.6 μm thick H_2O ice in the amorphous and crystalline phase.

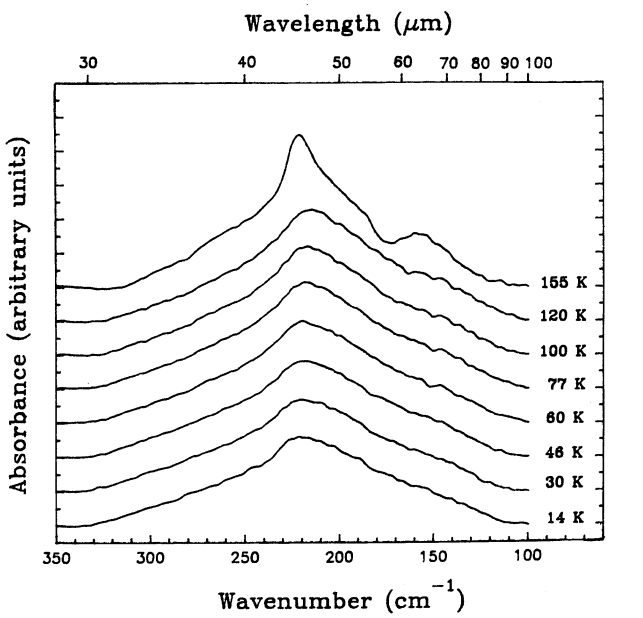

FIG. 3.—Far-infrared spectra of a 2.3 μm thick amorphous ice at different temperatures.

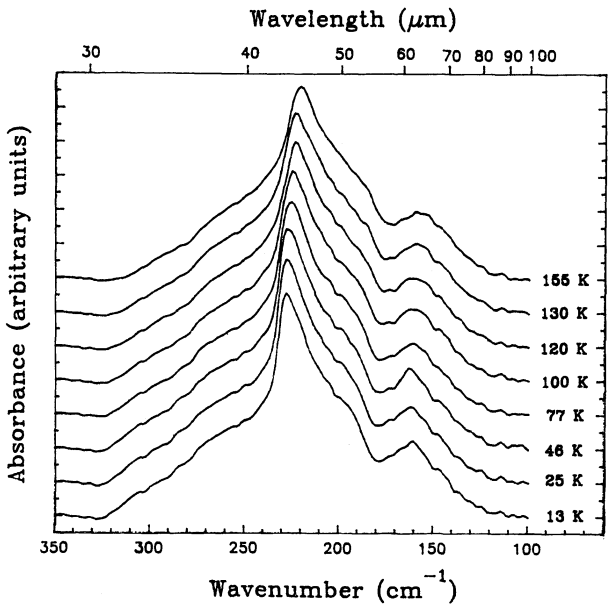

FIG. 4.—Far-infrared spectra of a 3.6 μm thick crystalline ice at different temperatures.

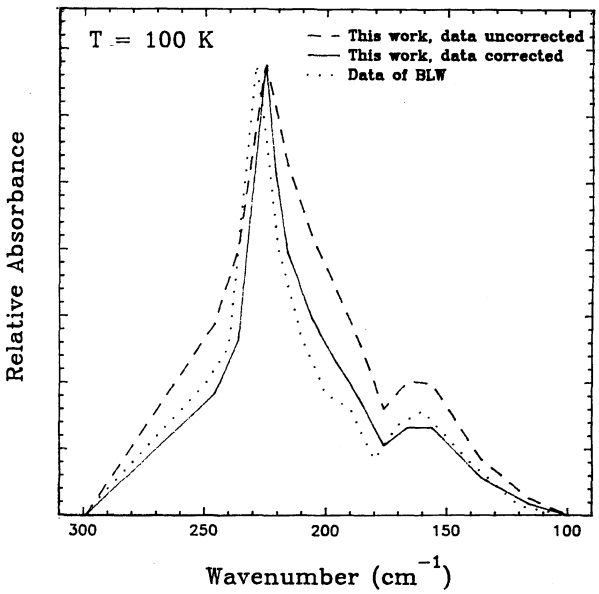

FIG. 6.—Comparison of far-infrared spectral data at 100 K. Our spectral data, uncorrected and corrected, are compared to data from BLW (see Bertie et al. 1969).

perature increases the peak position shifts to longer wavelengths; this change for amorphous ice is irreversible with temperature. The conversion to the crystalline form is complete at 155 K. Figure 4 shows the evolution of the far-infrared spectra of crystalline ice from 155 to 13 K. The peak positions of both maxima shift to shorter wavelengths as the temperature decreases. This change for crystalline ice is reversible with temperature. Therefore, the peak positions are directly related to the ice temperature. Changes in the peak positions with temperature for both amorphous and crystalline ice are summarized in Figure 5.

We compared our crystalline ice at 100 K with two sets of far-infrared data. Bertie et al. (1969) (referred to as BLW) published absorption coefficients calculated from transmission spectra (corrected for reflection losses) of crystalline ice formed by vapor condensation at 173 K on a polyethylene window. They published 16 values between 33 μm and 100 μm. Khanna (1992) measured transmission spectra of crystalline ice formed by annealing (to 150 K) vapor deposits condensed at 10 K on a polyethylene window. We normalized Khanna's data (which were uncorrected for reflection losses) to BLW's absorption coefficients at the principal maximum and found the area of the two curves between 33 μm and 100 μm differed by only ~3%. We therefore considered the shape and normalized areas of these curves as our standard.

The area of our TRT spectrum is 30% larger than BLW's data when normalized at the principal maximum. We attributed this to the fact that our spectrum resulted not only from detection of the attenuated component of the beam but also from the component reflected from the front surface of the ice. To correct for this, we used the reflectivity values of ice from BLW's data. The magnitude of the correction is proportional to the reflectivity of crystalline ice which (between 2.5 μm and 300 μm) reaches its maximum of 26.5% near 44 μm. Figure 6 shows the normalized spectrum after correction for reflection; its area is within a few percent of BLW's. Interference and phase effects have not been included in our corrections, but need to be considered in a more accurate modeling program we envision for future spectral comparisons. It has been recognized that differences can occur between the band strengths and band widths of transmission spectra and TRT spectra (e.g., Kitta & Krätschmer 1983). Since the magnitude of the problem is greatest for our far-infrared data, it is necessary to correct our TRT-spectra of crystalline H_2O before they can be directly compared with astronomical data. Corrected data at 100 K are available in digital form from the authors. The determination of the amorphization effects of irradiation on crystalline ice were all made using a self-consistent set of spectral data which did not have to be corrected for reflection losses.

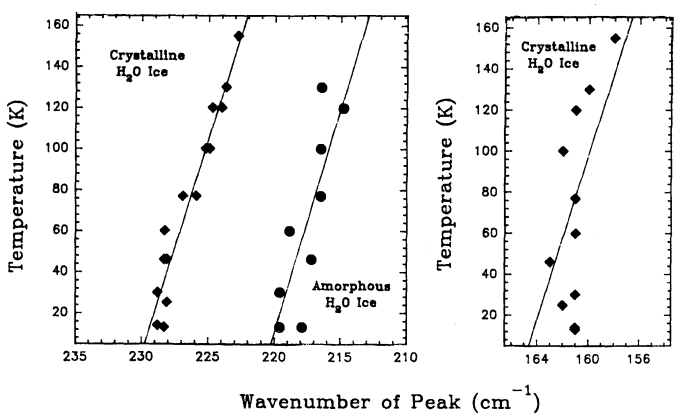

FIG. 5.—Peak positions of crystalline and amorphous ice as a function of temperature. A linear least-squares fit to the data points has been drawn for each maximum.

3.2. *Irradiation of H_2O Ice at 36 K < T ≤ 120 K*

Amorphization of crystalline ice due to 700 keV proton irradiation has been measured at temperatures from 77 K to 13 K. Figure 7 is the far-infrared spectra of 36 K crystalline ice before and after irradiation. For comparison, the dotted curve for

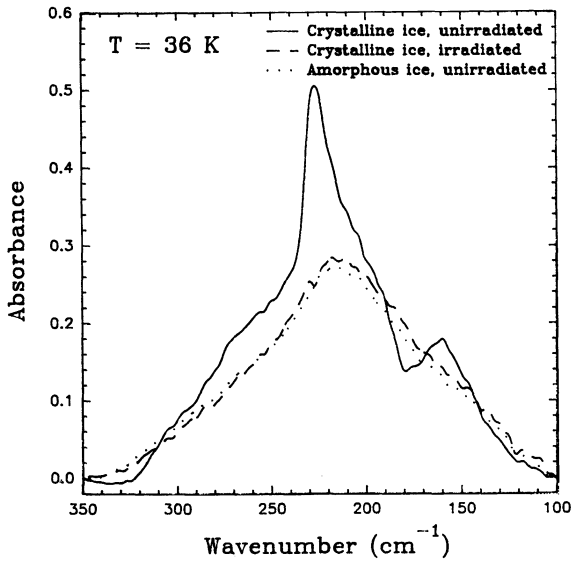

FIG. 7.—Far-infrared spectra of crystalline ice before and after irradiation

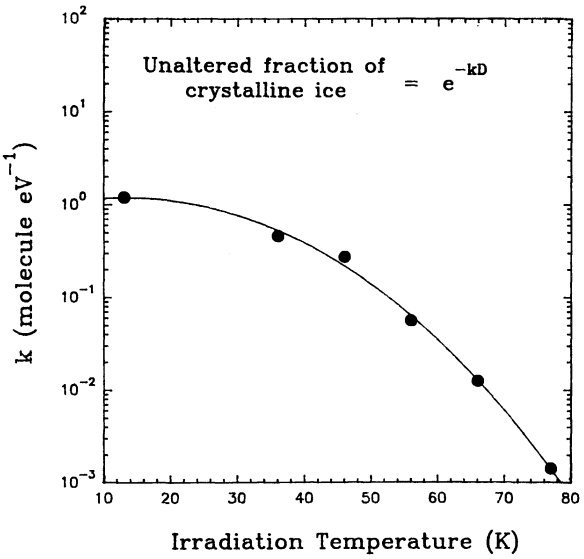

FIG. 9.—Dependence of k on temperature. "k" is a measure of the number of molecules converted from the crystalline to amorphous phase for each 1 eV molecule^{-1} dose. The line drawn through the data points shows a linear least-squares fit of (log K) to temperature.

irradiated amorphous ice at 36 K is nearly indistinguishable from unirradiated amorphized ice deposited at 13 K and warmed to 36 K. In this sample we estimate that the unaltered fraction of crystalline ice is 4% after a dose of 6 eV molecule^{-1}. To calculate the unaltered fraction, we assume that the spectrum after irradiation can be explained by a combination of only two components, some fraction of unaltered crystalline, f_C, and some fraction of amorphous ice, f_A. For example, at 36 K the absorbance of the principal maximum after irradiation is the sum of $f_C \times$ (maximum absorbance at 44 μm for unirradiated crystalline ice at 36 K) and $f_A \times$ (absorbance at 44 μm for the same thickness amorphous ice at 36 K). Unaltered fractions as a function of dose were calculated for spectra taken after the irradiation of ice at 13, 36, 46, 56, 66, and 77 K, and the results are plotted in Figure 8. Our longest duration experiment at 77 K lasted 5 hr. We estimate that during that time, less than 1% of any amorphous component could arise from direct condensation of residual water vapor inside the vacuum chamber.

The rate of change in the unaltered fraction of crystalline ice was fitted by a simple exponential law of the form

$$f_C = e^{-kD}, \quad (1)$$

where D is the dose and k is a temperature-dependent constant. The units of k are molecule eV^{-1}, and k represents the number of phase-converted molecules for a 1 eV molecule^{-1} dose at a particular temperature. Figure 9 plots calculated values of k for each experimental temperature. The number of phase-converted molecules near 77 K is two orders of magnitude less than the number at temperatures near 36 K. These results are in qualitative agreement with experiments involving ultraviolet irradiation (Kochi & Kuroda 1990), e^- irradiation (Lepault et al. 1983; Dubochet & Lepault 1984; Heide 1984), and He^+ irradiation (Strazzulla et al. 1991; Strazzulla 1991) of crystalline H_2O ice.

In contrast to these results for crystalline ice, our experiments on the irradiation of amorphous ice in the same temperature region gives virtually no detectable spectral changes. We did not detect changes in the amorphous ice during increased irradiation that we could attribute to an induced transition from low-density to high-density amorphous ice as was detected by Heide (1984) using electron diffraction. We also irradiated amorphous ice at temperatures as high as 125 K with ~40 eV molecule^{-1} and were not able to induce a crystalline phase transformation. Heide (1984) observed phase transformations from amorphous to crystalline ice at 120 K, but this was induced using very large doses of electron radiation (~2000 eV molecule^{-1}). Results from our experiments at temperatures lower than 36 K, however, showed radiation-induced changes in both crystalline and amorphous H_2O ice.

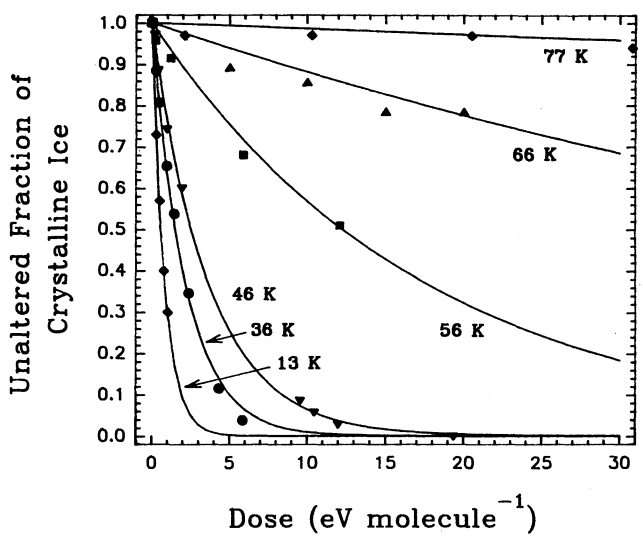

FIG. 8.—Unaltered fraction of crystalline ice at different temperatures as a function of dose.

3.3. *Irradiation of* H_2O *at* $T < 36$ K

The results are more complex after irradiation at lower temperatures. Figure 10 shows the spectrum of crystalline ice

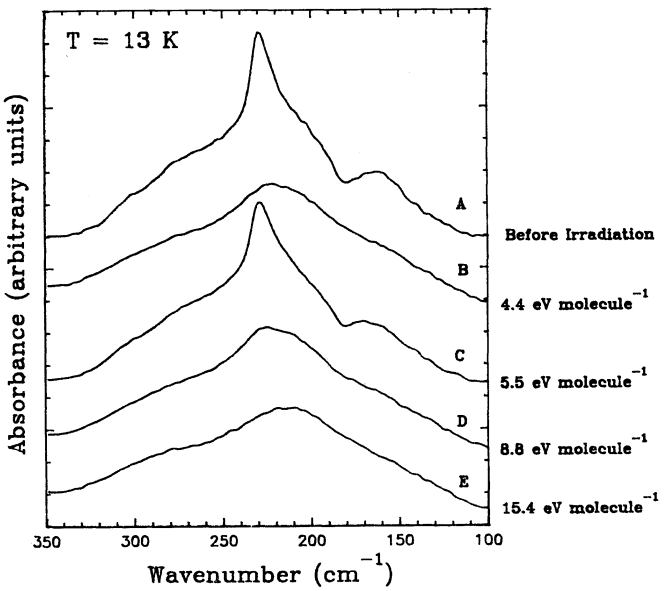

FIG. 10.—Irradiated crystalline ice at 13 K as a function of fluence. This sequence of spectra shows phase oscillations in H_2O ice induced by proton irradiation.

before irradiation (A) at 13 K. Spectra taken after three different radiation doses (B, C, D) show that the ice is oscillating between a crystalline and an amorphous phase. With additional irradiation the sample converts to a different amorphous ice (E) which resists further change. The peak position for spectrum (E) is 46.3 μm (211 cm^{-1}). No oscillations are detected at higher temperatures. We have observed, however, that some amorphous ice will crystallize during warming at temperatures as low as 46 K after irradiation at 13 K.

A mass spectrometer interfaced with the sample chamber detected bursts of material during the 13 K irradiations. The time display mode of the mass spectrometer gives a pressure versus time plot for up to five preselected ions. When the irradiation is first initiated, small sporadic bursts of predominately H_2 are observed, but after a dose of $\sim$2 eV molecule^{-1}, the bursts repeat with each additional dose of $\sim$1 eV molecule^{-1}. Figure 11 shows the occurrence of three such bursts and the relative intensity of the H_2, H_2O, OH, O_2, and H_2O_2 ion signals. Tick marks on the horizontal scale are 36 s apart, corresponding to a fluence of 4.5×10^{12} protons cm^{-2}. If the sample's spectrum is recorded immediately after a burst, it is always that of a crystalline ice. Spectra taken between bursts show that the ice is undergoing the crystalline-to-amorphous conversion. These regular bursts and accompanying ice recrystallizations are not seen at higher temperatures.

4. DISCUSSION AND CONCLUSIONS

4.1. *Mechanistic Considerations*

It is not surprising that crystalline H_2O ice can be amorphized by proton bombardment. Proton irradiation (Golecki & Jaccard 1978), electron irradiation (Heide 1984; Lepault et al. 1983), He^+ irradiation (Strazzulla et al. 1991; Strazzula 1991), and *uv* photolysis (Kouchi & Kuroda 1990) have all been reported to amorphize crystalline ice. In each of these cases, and in our own work, the particle/photon dose needed to amorphize the ice varied inversely with temperature. These observations can be most easily understood by considering the products formed by the radiation and their subsequent fate.

Although the radiation chemical products of ice have not been studied in exhaustive detail, they can be inferred from experiments in the literature. Stable ions such as H_3O^+ and OH^- are expected, based on the radiation chemistry of water (Klassen 1987). Electron spin resonance (ESR) spectra of crystalline ice irradiated at 4.2 K show H and OH free radicals. Warming above $\sim$20 K causes essentially complete H decay by 77 K but little, if any, OH decay (Johnson & Moulton 1978; Flourney, Baum, & Siegel 1962; Hase & Kawabata 1976). Electrons, ejected from water molecules during ionization, could be trapped in the ice but this is not expected to be important in our samples. ESR experiments of X-irradiated (Johnson & Moulton 1978) and γ-irradiated crystalline (Flournoy et al. 1961; Hase & Kawabata 1976) and amorphous H_2O ices (Marx, Leach, & Horani 1963) show, at best, only a very weak trapped electron signal. We know of no direct evidence for production of O, O_2, and H_2O_2 products at $\sim$13 K. Sputtering experiments have demonstrated H_2 production at 10 K (Reimann et al. 1984) and mass spectrometry shows extensive H_2 release between 15 and 70 K (Kouchi & Koroda 1990; Laufer, Kochavi, & Bar-Nun 1987).

A mechanism or model is desirable for the following observations: (1) the conversion of crystalline H_2O ice into amorphous ice, (2) the temperature dependence of the conversion, and (3) the cycling that occurs between the crystalline and

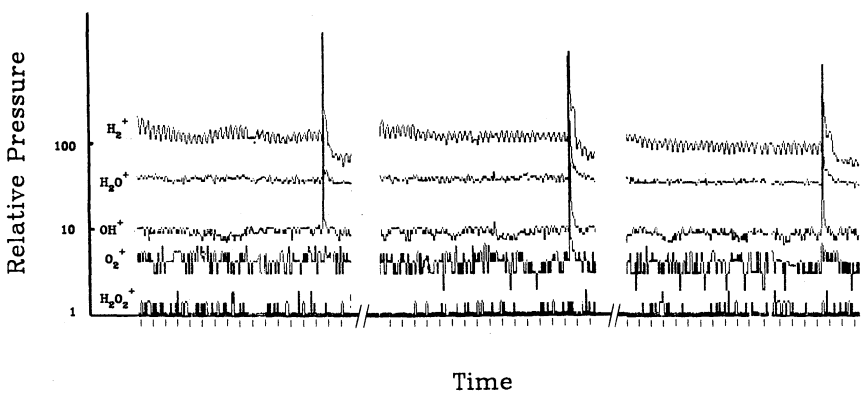

FIG. 11.—Relative pressure of five masses released during radiation H_2O ice at 13 K as a function of time. Tick marks on the horizontal scale are 36 s apart, corresponding to a fluence of 4.5×10^{12} protons cm^{-2}. Three large bursts of material are shown; they occur after a dose of $\sim$1 eV molecule^{-1}.

amorphous phases at 13 K. We first assume that the incident 700 keV protons produce excitations and ionizations in the ice samples which ultimately lead to H_3O^+, OH^-, H, OH, H_2, as well as other species. It is the accumulation of these products which causes the ice to lose its initially crystalline nature and become increasingly amorphous.

Atomic and molecular hydrogen, H and H_2, are especially significant for explaining why increasingly larger radiation doses are needed to amorphize the ice as the temperature is raised. H_2 will be retained at ~ 13 K but a substantial quantity will sublime in the 15–70 K region. H can be lost by the reactions below:

$$H + H \rightarrow H_2 , \quad (2)$$

$$H + OH \rightarrow H_2O . \quad (3)$$

It is at the lowest temperatures that H_2 and H are most efficiently stored in the ice, and therefore the amorphization rate is largest. As the temperature is raised, increasingly larger radiation doses are needed to counter the tendency of H to react and H_2 to sublime, tendencies that will make the ice appear more "radiation resistant," as was observed.

The final point to be explained is the cycling of the H_2O ice between the crystalline and amorphous phases along with the associated release of material. This behavior is most pronounced at ~ 13 K which suggests that trapped H and H_2 play important roles. Similarly, Fontana (1959) and Windsor (1961) reported bursts of material during depositions at 4.2 K of streams of N_2 that had been passed through a microwave discharge to produce free radicals. Bursts of material were observed as the samples grew in thickness and the number of deposited radicals increased. Jackson (1959a, b) developed models and derived equations for both the maximum number of free radicals that could be stored and the sample thickness required for stability. Jackson's model contains many unknowns, however, which makes it difficult to directly apply to our experiments. Nevertheless, we suggest that H accumulates in our ices during irradiation at 13 K until some critical concentration is reached. At that point a burst of material is detected as radical combination reactions occur. The energy released causes a recrystallization of the ice. Bursts are not expected at higher temperatures since H will not accumulate as rapidly, as explained above, and indeed such bursts are not seen. Phase cycling was not reported by Strazzulla et al. (1991) and Strazzulla (1991) who irradiated 10 K ice samples 100 times thinner than ours with He^+. It is possible that H accumulation is affected by the ice thickness. A more detailed discussion of the behavior of irradiated amorphous ice at $T < 36$ K is given in Hudson & Moore (1992).

We plan to search for amorphous-crystalline cycling in mixed ices, such as CO + H_2O, in the future. It would also be interesting to see if the effect is dependent on ice thickness since Strazzulla et al. (1991) and Strazzulla (1991) do not report cycling their irradiated ices.

4.2. *Astronomical Implications*

Our results are in qualitative agreement with published data on the amorphization of crystalline water ice by ultraviolet photolysis (Kouchi & Kuroda 1990), and electron irradiation (Dubochet et al. 1982; Lepault et al. 1983; Heide 1984). In those experiments the diffractograms detected the structural change from crystalline to amorphous ice, but not the rate of amorphization.

Our proton irradiation results also qualitatively agree with Strazzulla et al. (1991) and Strazzulla (1991) since we find that the rate of amorphization increases with decreasing temperature. Strazzulla (1991) measured changes in the 3.1 μm absorption band of crystalline water ice as a function of He^+ irradiation at different temperatures and calculated the fraction of amorphous ice formed in the crystalline ice as a function of dose. For example, in both our experiments and Strazzulla's the deposited energy required to convert 50% of the crystalline ice at 36 K to the amorphous phase is near 1 eV molecule^{-1} to 2 eV molecule^{-1}. At temperatures higher than this, however, it becomes difficult to compare results. The general trend of Strazzulla's data shows that above ~ 50 K (for a specific dose), a larger fraction of crystalline ice is altered than in our proton-irradiated ice. We are unable to attribute this to the difference between He^+ and H^+ rate of energy transfer to the ice. What is certain is that ion, and presumably photon and electron, induced amorphization of ice at temperatures below 70 K modifies both the 3.1 μm and far-infrared absorption features of crystalline H_2O ice until they are indistinguishable from those of amorphous ice. Therefore we emphasize that the detection of amorphous ice is not sufficient to determine the formation and/or storage temperature of the material.

A source of proton irradiation for interstellar materials is low-energy cosmic-ray protons. Flux estimates are sometimes based on the assumption that the state of ionization observed for trace elements in interstellar gas is a measure of the cosmic-ray flux. If we use 10 cm^{-2} s^{-1} (e.g., Calcagno, & Foti 1983) for protons with energies near 1 MeV, then an interstellar icy grain would experience 3×10^{14} protons cm^{-2} in 10^6 yr. The rate of deposit of energy for a 0.7 MeV proton in H_2O ice is 1.3×10^{-14} cm^2 eV molecule^{-1} (Northcliffe & Schilling 1970). Therefore, the energy deposited in the ice is near 4 eV molecule^{-1}, an amount sufficient to amorphize more than 50% of the crystalline ice stored at temperatures up to near 50 K in 10^6 yr. At a 50% conversion the spectrum is noticeably different from that of pure crystalline or pure amorphous ice.

Cosmic-ray irradiation of ice in IRAS 09371+1212 is expected along with some contribution from ultraviolet photons. Kouchi & Kuroda (1990) estimated time scales for amorphization due to ultraviolet photons could be 10^5 yr in dense molecular clouds (this depends on the ultraviolet extinction in the cloud). Another source of radiation in nebular regions such as IRAS 09371+1212 may result from the large mass losses (and accompanying large outflow velocity) experienced by these evolving stars. Baratta et al. (1991) discussed this type of source for keV H^+ ions in OH 231.8+4.2. If we assume all of these sources are present in IRAS 90371+1212, then the time required to convert 50% of crystalline ice to the amorphous phase would be much less than 10^6 yr. Omont et al. (1990) point out that the narrowness of the 45 μm feature in IRAS 90371+1212 fits the narrow crystalline ice spectrum and that the fit is not as good if a 50% crystalline and 50% amorphous ice spectrum is used. If we assume the ice is crystalline because it has not been exposed long enough in a nebulae's radiation environment we can use the results of our experiments to give an upper age limit of 10^6 yr. This age is consistent wth a calculated upper limit based on the observed size of the nebula and its estimated distance from us.

Amorphous ice appears to be radiation resistant between 20 and 125 K. The only exception to this is in some electron-beam experiments where crystallization is observed above 120 K, but

the required energy doses are so large that the results do not seem astrophysically relevant. It is not known, however, if the radiation-induced conversion of amorphous to crystalline ice can be altered by the presence of icy mixtures, by radiation residues in the ice, or by the inclusion of materials such as silicates. We have also observed some amorphous ice to crystallize during warming at temperatures as low as 46 K after it has been irradiated at 13 K. These experiments are especially applicable to cometary chemistry. The nuclei of new comets are expected to be amorphous ice which have been subjected to cosmic-ray irradiation. The crystallization of the surface layers (and the accompanying large increase in the thermal conductivity) could occur at even lower temperatures (greater distances from the Sun) than previously predicted if our results also apply to more relevant cometary type icy mixtures.

Our observation of the irradiation-induced phase cycling of both amorphous and crystalline ice at 13 K means that the identification of the phase of interstellar water ice is not sufficient information for determining its formation temperature or thermal history. The detection of H_2, H_2O, and O_2 during the phase cycling suggests that similar releases may occur in irradiated cosmic icy mixtures. Phase cycling is expected to reduce the number of reactive species stored at 13 K and to affect the radiation yield and storage of complex molecules. Experiments designed to detect these effects in icy mixtures are in progress.

A possible additional effect is that the spin temperature (a parameter related to the ortho-para ratio, OPR) may be affected by the phase oscillations since both the release of gas during phase cycling, and the synthesis of O_2 (a paramagnetic species) occur. It has been suggested that the OPR could be used as a tracer of the origin and evolution of comets (Mumma, Weissman, & Stern 1992). Water from comets is expected to show a relaxed OPR (a value less than the equilibrium ratio of 3) if the water formed originally in a low-temperature region (T below 50 K). The result for comet Halley was an OPR = 2.5, equivalent to a spin temperature of 29 K (Mumma, Weaver, & Larson 1987). From our experiments we know that only a few eV molecule^{-1} (equivalent to $\sim 10^5$ yr interstellar exposure) is required to drive the cycling behavior we observed at 13 K which may reset the OPR. Therefore, it may be possible to accrete cometesimals from phase-cycled ices at $T < 20$ K which exhibit a higher spin temperature than cometesimals accreted from ices where $T > 20$ K.

We thank B. Donn for many helpful discussions related to our experiments. We acknowledge R. Khanna at University of Maryland who provided unpublished water spectra and Hudgins, Sandford, Allamandola, and Tielens at NASA/Ames Research Center who made available optical constants prior to publication. We thank Steve Brown and members of the GSFC/Radiation Facility for operation of the accelerator. R. Hudson acknowledges the Administration of Eckerd College for a leave under which this work was done through an Intergovernmental Personnel Act Agreement with NASA/GSFC. Both authors acknowledge NASA funding support of grant NSG 5172.

REFERENCES

Baratta, G. A., Leto, G., Spinella, F., Strazzulla, G., & Foti, G. 1991, A&A, 252, 421
Bertie, J. E., & Jacobs, S. M. 1977, J. Chem. Phys., 67, 2445
Bertie, J. E., Labbé, H. J., & Whalley, E. 1969, J. Chem. Phys., 50, 4501 (BLW)
Bertie, J. E., & Whalley, E. 1967, J. Chem. Phys., 46, 1271
Dubochet, J., Lepault, J., Freeman, R., Berriman, J. A., & Homo, J.-C. 1982, J. Microsc., 128, 219
Dubochet, J., & Lepault, J. 1984, J. de Physique, 45, C7-85
Eiroa, C., & Hodapp, K. W. 1989, in Proc. of 22nd Eslab Symp. ESA, ed. B. H. Kaldeich (SP-290), 351–353
Flournoy, J. M., Baum, L. H., & Siegel, S. 1961, J. Chem. Phys., 34, 1782
Fontana, G. 1959, J. Chem. Phys., 31, 148
Geballe, T. R., Kim, Y. H., Knacke, R. F., & Noll, K. S. 1988, ApJ, 326, L65
Golecki, I., & Jaccard, C. 1978, J. Glaciology, 21, 247
Hardin, A. H., & Harvey, K. B. 1973, Spectrochimica Acta, 29A, 1139
Hase, H., & Kawabata, K. 1976, J. Chem. Phys., 65, 64
Heide, H. G. 1984, Ultramicrosc., 14, 271
Hobbs, P. V. 1974, in Ice Physics (Oxford: Clarendon), 60
Hodapp, K. W., Sellgren, K., & Nagata, T. 1988, ApJ, 326, L61
Hudgins, D. M., Sandford, S. A., Allamandola, L. J., & Tielens, A. G. G. M. 1992, J. Phys. Chem. Ref. Data, submitted (HSAT)
Hudson, R. L., & Moore, M. H. 1992, J. Phys. Chem., 96, 6500
Jackson, J. L. 1959a, J. Chem. Phys., 31, 154
———. 1959b, J. Chem. Phys., 31, 722
Johnson, J. E., & Moulton, G. C. 1978, J. Chem. Phys., 69, 3108
Jura, M., & Morris, M. 1985, ApJ, 292, 487
Khanna, R. 1992, private communication
Kitta, K., & Krätschmer, W. 1983, Astr. Ap., 122, 105
Klassen, N. V. 1987, in Radiation Chemistry, ed. Farhataziz & M. A. J. Rodgers (New York: VCH Publishers)
Klinger, J. 1983, J. Phys. Chem., 87, 4209
Kouchi, A., & Kuroda, T. 1990, Nature, 344, 134
Laufer, D., Kochavi, E., & Bar-Nun, A. 1987, Phys. Rev. B, 36, 9219
Léger, A., Gauthier, S., Défourneau, D., & Rouan, D. 1983, A&A, 117, 164
Lepault, J., Freeman, R., & Dubochet, J. 1983, J. Microsc., 132, RP3
Marx, R., Leach, S., and Horani, M. 1963, J. Chim. Phys., 60, 726
Mumma, M. J., Weaver, H. A., & Larson, H. P. 1987, A&A, 187, 419
Mumma, M. J., Weissman, P. R., & Stern, S. A., 1992, in Protostars and Planets III, ed. E. H. Levy, J. I. Lunine, & M. S. Matthews (Tucson: Univ. of Arizona Press), in press
Narten, A. H., Venkatesh, C. G., & Rice, S. A. 1976, J. Chem. Phys., 64, 1106
Northcliffe, L. C., & Shilling, R. F. 1970, Nuclear Data Tables, A7, 233
Omont, A., Moseley, S. H., Forveille, T., Glaccum, W. J., Harvey, P. M., Likkel, L., Loewenstein, R. F., & Lisse, C. M. 1990 ApJ, 355, L27
Reimann, C. T., Boring, J. W., Johnson, R. E., Garrett, J. W., Farmer, K. R., Brown, W. L., Marcantonio, K. J., & Augustyniak, W. M. 1984, Surface Sci., 147, 227
Rouan, D., Omont, A., Lacombe, F., & Forveille, T. 1988, A&A, 189, L3
Smith, R. G., Sellgren, K., & Tokunaga, A. T. 1988, ApJ, 334, 209
Strazzulla, G. 1991, in 2nd Internat. Workshop on The Nature of Cometary Organic Matter, Asilomar, CA
Strazzulla, G., Calcagno, L., & Foti, G. 1983, MNRAS, 204, 59
Strazzulla, G., Leto, G., Baratta, G. A., & Spinella, F. 1991, J. Geophys. Res., 96, 17, 547
Windsor, M. W. 1961, in Fifth International Symp. on Free Radicals (New York: Gordon & Breach), 73-1